Performance of a radial-inflow turbine integrated in an ORC system and designed for a WHR on truck application: An experimental comparison between R245fa and R1233zd

ARTICLE · MARCH 2016

DOI: 10.1016/j.apenergy.2016.03.012

Applied Energy xxx (2016) xxx–xxx

Contents lists available at ScienceDirect

Applied Energy

journal homepage: www.elsevier.com/locate/apenergy

Performance of a radial-inflow turbine integrated in an ORC system and designed for a WHR on truck application: An experimental comparison between R245fa and R1233zd

Ludovic Guillaume *, Arnaud Legros, Adriano Desideri, Vincent Lemort

Thermodynamics Laboratory, University of Liège, Campus du Sart Tilman, B49, B-4000 Liège, Belgium

HIGHLIGHTS

- A WHRORC test rig integrating a radial inflow turbine is built.
- Performance of the system is evaluated for two working fluids: R245fa and R1233zd.
- Three types of experimental comparisons are proposed.
- *R1233zd* represents a better choice compared to *R245fa* for the current application.

GRAPHICAL ABSTRACT

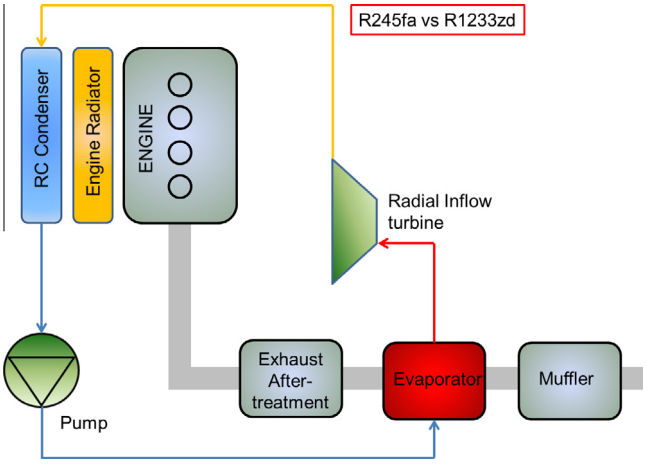

ARTICLE INFO

Article history:
Received 21 December 2015
Received in revised form 28 February 2016
Accepted 6 March 2016
Available online xxxx

Keywords:
Waste heat recovery
Organic Rankine Cycle
Experimental comparison
Radial inflow turbine
Working fluid
R245fa and R1233zd

ABSTRACT

The goal of this study is to experimentally compare the performance of an Organic Rankine Cycle (ORC) system equipped with a radial-inflow turbine for two working fluids: R245fa and R1233zd. The radial-inflow turbine is a small-scale prototype designed to convert the waste heat from the exhaust gases of a truck combustion engine and was developed mainly using components of truck turbochargers. It is directly connected to a high-speed synchronous generator. The bearings system of the turbine and the generator have the innovative particularity to be respectively lubricated and cooled down by the working fluid so no additional lubricant or coolant is needed. The experimental comparison is carried out over a test-rig equipped with the radial turbine. The heat wasted by the truck through the exhaust gases is simulated using an electric oil boiler coupled to the ORC loop. The electrical power supplied by the turbine, limited to a maximum of 3.5 kWel by the generator, is then dissipated in a load bank composed of truck fans while the condenser is cooled by a water loop. Measurements in steady-state are performed in order to evaluate the performance of the turbine-generator set when varying the pressure ratio, the rotational speed, the inlet temperature and the mass flow rate of the turbine and the lubrication flow rate of the

* Corresponding author.
E-mail address: ludovic.guillaume@ulg.ac.be (L. Guillaume).
URL: http://www.labothap.ulg.ac.be (L. Guillaume).

http://dx.doi.org/10.1016/j.apenergy.2016.03.012

Nomenclature

Acronyms

APS	absolute pressure sensor
CFM	Coriolis flow meter
GHG	GreanHouse Gases
GWP	Global Warming Potential
ODP	Ozone Depletion Potential
ORC	Organic Rankine Cycle
PP	pinch point
TIT	Turbine Inlet Temperature
WHR	Waste Heat Recovery

Subscripts

cd	condenser
cf	cold fluid
el	electrical
ev	evaporator
ex	exhaust
exp	expander
hf	hot fluid
HP	high pressure
l	liquid
LP	low pressure
pp	pump
rec	recuperator
s	isentropic
sc	sub-cooled
sh	super-heated
su	supply
sub	subcooler
tur	turbine
v	vapor

Symbols

c_p	spec. heat capacity (kJ/kg K)
Δ	difference
η	efficiency
ε	efficiency
h	spec. enthalpy (kJ/kg)
$\dot{m}$	mass flow (kg/s)
p	pressure (bar)
$\dot{Q}$	Thermal power (kW)
T	temperature (°C)
V_r	Volume ratio (–)
$\dot{W}$	Electrical power (kW)

bearings for various oil temperatures and mass flow rates. In order to identify the most suitable fluid for the Waste Heat Recovery (WHR) application, three comparison methods are proposed and discussed based on the measurements. Finally, because the turbine-generator set is the first oil-free prototype developed by the manufacturer, potential sources of improvements are discovered and discussed.

1. Introduction

It is now accepted that emissions of greenhouse gases (GHG) from human activities are enhancing the global warming effect keeping the earth at a temperature higher than it would otherwise be [1]. In the last twenty years, the world energy consumption has increased by more than 30% [2] despite the adoption by the United Nations on Climate Change of the Kyoto Protocol [3].

Alone, the EU is responsible for around 10% of the global emissions of greenhouse gases. Nearly 80% of these emissions come from the production and use of energy and transport [4]. Looking at the situation as it was in 2012 in Europe in terms of GHG emissions (Fig. 1a), it can be seen that the transport sector is responsible of about one fifth of these emissions. It is also pointed out by the european commission that "*Heavy-Duty Vehicles (HDV) represent about a quarter of EU road transport* CO_2 *emissions and some 6% of the total EU emissions* [5]".

For a long time, the EU has stressed the need to limit global warming to 2 °C maximum. However, despite recent improvements in fuel consumption efficiency, HDV emissions are still rising, mainly because of the increasing number of vehicles in traffic. Nowadays, HDV are the second-biggest source of CO_2 emissions within the transport sector, i.e. larger than both international aviation and shipping. As a result, the reduction of the CO_2 emissions from HDV has become a strategic goal of the EU. "*As part of the EU's future strategy to address HDV fuel consumption and* CO_2 *emissions, a number of actions can be considered that will result in*:

- improved vehicle efficiency through new engines, materials and design,
- cleaner energy use through new fuels and propulsion systems,
- better use of networks and more efficient fleet operation, with the support of information and communication systems. [5]"

A very promising solution is the re-use of the waste heat, which is about 60% of the combustion energy. Transforming this heat in mechanical or electrical energy will enable to increase the overall energy efficiency of the vehicle. Consequently, the fuel consumption and the CO_2 emissions will be reduced.

The heat re-use can be performed by means of a thermodynamic cycle (e.g. organic or non-organic Rankine cycles) using the waste heat as energy source as it is being adopted for large stationary applications.

However the adoption of such technology in the automotive domain requires specific R&D activities to identify the most appropriate system architecture and integration level so to achieve sustainable cost and the reliability requirements. Among other, the transient behavior of the engine, the selection of the heat sources, the limited additional heat rejection capacity of the truck, the use of the energy produced by the expansion machine and the impact on the engine of the back pressure caused by the evaporator [6] are as many challenges to overcome during the design of the WHR system.

A major part of these research activities is also specially dedicated to the selection of the working fluid and of the expansion machine. The working fluid selection process has been widely investigated in several studies [7–11]. For instance, Macian et al. [12] selected R245fa and water for their optimization of a bottoming Rankine cycle. Nonetheless no universal optimal fluid is indicated since the choice is highly dependent on the target

Please cite this article in press as: Guillaume L et al. Performance of a radial-inflow turbine integrated in an ORC system and designed for a WHR on truck application: An experimental comparison between R245fa and R1233zd. Appl Energy (2016), http://dx.doi.org/10.1016/j.apenergy.2016.03.012

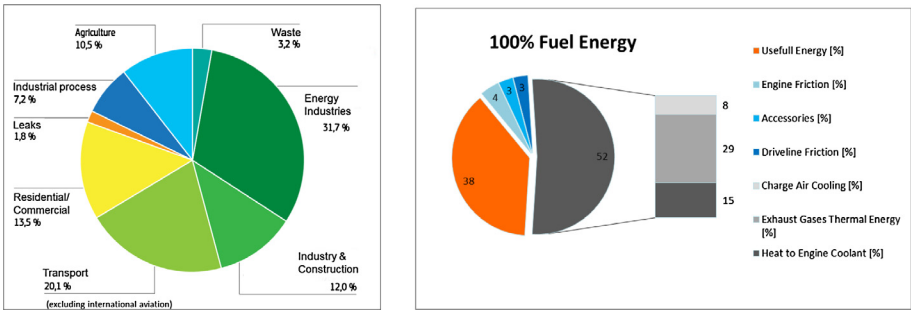

(a) European GHG emissions by sector in 2012. [4]

(b) Waste heat repartition for truck applications.

Fig. 1. Context of the WHR on HDV through ORC systems.

application. A detailed list of the guidelines and indicators that should be taken into account when selecting an organic fluid for power generation are reported in [13].

Several couples of working fluid and expansion machine used in ORC systems to recover the waste heat from vehicles also have been considered in literature. Zheng et al. investigated a rolling piston to recover the waste heat of a low temperature (90°C) heat source [14]. Costall selected toluene in a design methodology of a radial turbo expander [15]. Song et al. considered a screw expander using water for the LT loop in the analyze of the performance of a dual-loop ORC [16]. Di Battista et al. investigated a rotary vane expander using R236fa for the waste heat recovery of a light duty engine [17].

A significant number of studies dedicated to the waste heat recovery on trucks using Organic Rankine Cycles systems is also available [18–22] but only a few of them are considering experimental investigations [23,24].

In the present study, an experimental campaign is achieved to compare the performance of an ORC system equipped with a radial-inflow turbine for two working fluids: R245fa and its probable substitute R1233zd.

The turbine is an innovative small-scale prototype designed to convert the heat wasted in the exhaust gases and recirculated gases (EGR) of a truck. It was developed mainly using components of truck turbochargers and it is directly connected to a high-speed synchronous generator. The bearings system of the turbine and the generator have the particularity to be respectively lubricated and cooled down by the working fluid so no additional lubricant or coolant is needed.

A test rig integrating the turbine was built where the heat wasted by the truck through the exhaust gases is simulated using an electric oil boiler associated with the ORC loop. The electrical power supplied by the turbine, limited to a maximum of 3.5 kWe by the generator, is then dissipated in a load bank composed of truck fans while the condenser is cooled by a water loop.

Measurements in steady-state are performed in order to evaluate the performance of the turbine-generator set when varying the pressure ratio, the rotational speed, the inlet temperature and the mass flow rate of the turbine and the lubrication flow rate of the bearings for various oil temperatures and mass flow rates.

The cycle operates between a maximum heat source temperature of 180 °C and a minimum heat sink temperature of 10 °C. Based on the measurements, the thermodynamic performance of the ORC unit are evaluated and compared for the two fluids.

A particular attention is dedicated to the analysis of the turbine-generator set which is a key component in affecting the performance of the ORC unit. The other ORC components are classical components used in refrigeration systems and are not representative of the truck application. The impact on the engine of the back-pressure caused by the pressure drop in the evaporator can obviously not be measured and there is no limit on the condenser heat rejection.

Three methods of experimental comparison are established and discussed in order to identify the most suitable fluid:

- A first comparison between the fluids is achieved for same evaporating and condensing temperature levels. This is an objective comparison of the two fluids in case of exact same heat sources and heat sinks temperatures and mass flow profiles.
- A second comparison between the fluids is performed for same condensing temperature and evaporating pressure levels. This comparison is adapted to the waste heat recovery application where the evaporating pressure can be optimized if it is not limited by the temperature and mass flow rate conditions of the heat source.
- A comparison between the fluids for same evaporating and condensing pressure levels that allows in identifying the impact of the used working fluid on the turbine performance.

Finally, potential sources of improvements are discussed based on the experimental measurements, the oil-free turbine-generator prototype being the first of the kind developed by the manufacturer.

2. Materials and methods

2.1. ORC system

A schematic and a picture of the layout of the ORC test rig are given in Fig. 2a and c respectively. The system is equipped with the prototype of turbine-generator set.

The radial-inflow turbine itself consists of three main parts, the volute, the stator and the rotor as depicted in Fig. 2b. Thus, the incoming fluid is accelerated and distributed uniformly around the periphery of the stator by the volute. Further acceleration and increase in the circumferential component of velocity is provided by the stator which is constituted of nozzles. Then the kinetic energy of the fluid is converted into mechanical energy as it expands through the rotor [25]. This turbine was developed mainly using components of truck turbochargers and directly coupled to a high speed electrical generator. In order to achieve the lubrication of the bearings system and the cooling of the generator with the working fluid, two lines go directly from the pump outlet to the bearings and generator casings respectively, in parallel to the main flow driven to the evaporator, as shown in Fig. 2a.

The variable speed membrane pump, through an asynchronous generator, is connected to an inverter that allows controlling the

Please cite this article in press as: Guillaume L et al. Performance of a radial-inflow turbine integrated in an ORC system and designed for a WHR on truck application: An experimental comparison between R245fa and R1233zd. Appl Energy (2016), http://dx.doi.org/10.1016/j.apenergy.2016.03.012

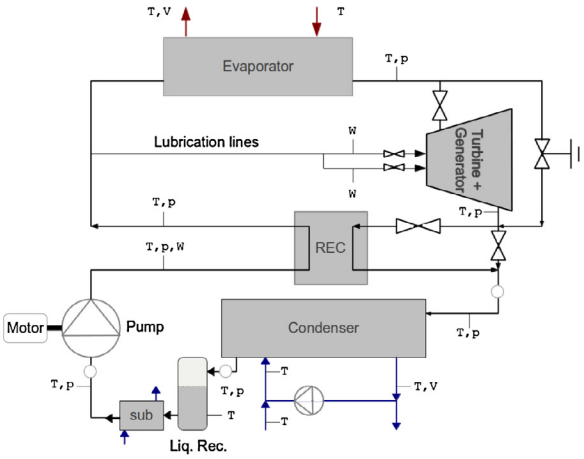

(a) Schematic layout of the ORC test rig

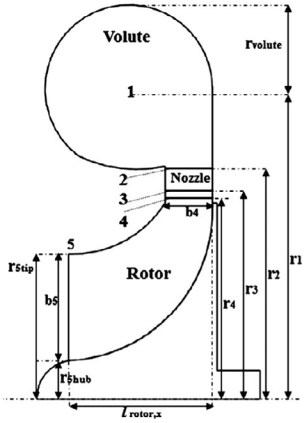

(b) Schematic of the radial turbine meridional view [25]

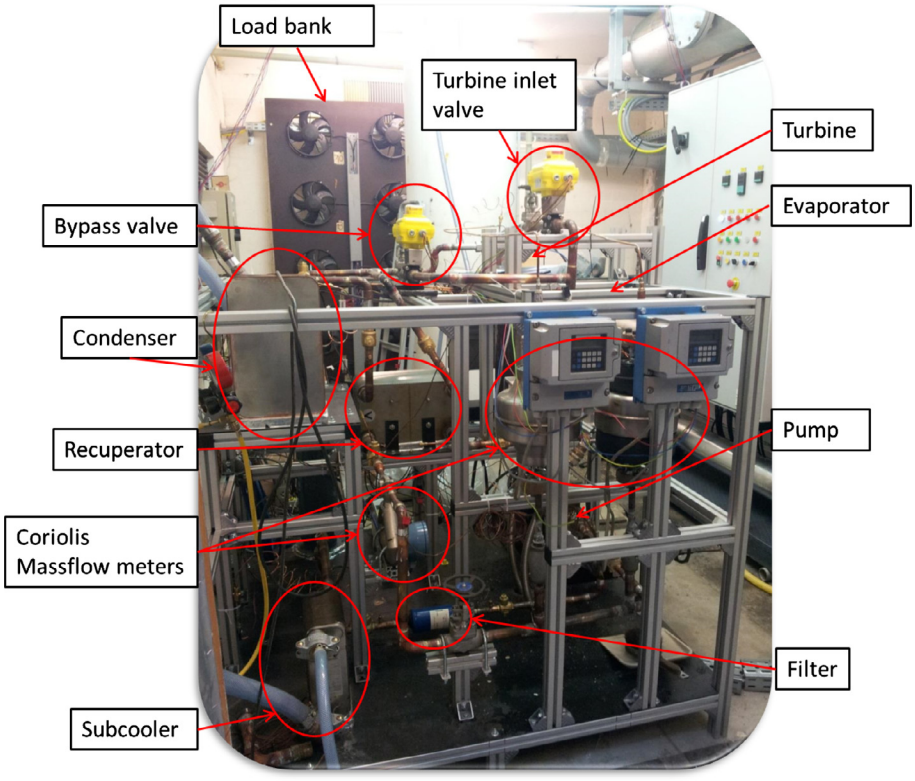

(c) Picture of the ORC test rig

Fig. 2. Description of the experimental setup.

rotational speed of the machine. The waste heat is simulated using an electric oil boiler coupled to the ORC loop. The electrical power, produced by the turbine generator and limited to 3.5 kWe, is dissipated in a load bank composed of truck fans while the condenser is cooled by a water loop. A liquid receiver is placed between the condenser outlet and the subcooler inlet to ensure a sufficient height of liquid at the inlet of the pump.

A summary of the main ORC components characteristics is reported in Table 1. The working fluid in liquid stated is pumped and split in three lines. The main part of the high pressure liquid is driven to the evaporator to recover the heat provided by the thermal oil of the boiler. The resulting high pressure vapor is then expanded in the turbine where the thermal energy is converted in mechanical energy and then electrical energy through the high speed generator. The remaining liquid coming from the pump is driven to the turbine bearings and the generator to respectively lubricate and cool down these components.

Please cite this article in press as: Guillaume L et al. Performance of a radial-inflow turbine integrated in an ORC system and designed for a WHR on truck application: An experimental comparison between R245fa and R1233zd. Appl Energy (2016), http://dx.doi.org/10.1016/j.apenergy.2016.03.012

Table 1
Summary of the specifications of the main ORC unit components.

System component	Specifications
Heat exchangers	Brazed plate type T_{max} = 180 °C, P_{max} = 30 bar
Pump	Volumetric Membrane pump 3 kW motor, N_{nom} = 1500 rpm, P_{max} = 70 bar
Expansion machine	Radial turbine 3.5 kW generator, $\dot{M}$ = 0–350 g/s, r_p = 2–5 [–], N = 50,000–80,000 rpm $\dot{M}_{lub}$ = 0.04–0.1 [kg/s]
Liquid receiver	8 l

The three aforementioned flows are combined afterward before entering the condenser where the fluid goes back to saturate liquid state based on the heat exchange with the cooling water.

The saturated liquid finally fills the liquid receiver, in which the accumulated mass of liquid enables to dump the transient variations occurring during the operation of the system, before being further cooled down in the subcooler. This ensure the fluid is in a low temperature liquid state at the inlet of the pump and thus avoid cavitation.

2.2. Heating and cooling loops

The low-capacity waste heat thermal energy source is represented by means of an electrical boiler where thermal oil, Pirobloc HTF-Basic, is pumped through to temperatures of up to 300 °C. The boiler has a maximum power of 150 kW_{th}. A proportional integral (PI) controller is implemented to maintain the temperature of the oil at the inlet of the evaporator constant during transient in the ORC test rig (e.g. change in the pump rotational speed of the ORC). The oil mass flow rate provided by the boiler being too large for the ORC application, it is manually controlled through a by-pass loop by means of needle valves located at the inlet of the evaporator.

A variable flow rate of water is used as heat sink to cool down the working fluid in the condenser (and the subcooler).

2.3. Data acquisition systems

On the working fluid side, absolute pressure sensors (APS) and Type-T thermocouples at the inlet and outlet of the different components allow for the determination of the energy balance for each component and the management of the plant. The working fluid mass flow rates are measured by means of three Coriolis flow meters (CFM) installed in parallel at the pump outlet.

The condenser cooling loop is equipped with two type-T thermocouples to measure the temperature of the cooling fluid at the inlet and outlet of the water side and a water counter is used to measure the flow rate of water.

Table 2
Range and precision of the measurement devices.

Variable	Device type	Range	Uncertainty
Mass flow	CFM	0–0.5 kg/s	±0.1%
T (ORC)	type-T thermocouples	0–150 °C	±0.5 K
T (heat sink)	type-T thermocouples	0–15 °C	±0.5 K
T (heat source)	type-K thermocouples	0–180 °C	±1.5 K
p	APS	0–30 bar	±0.03 bar
El. Power	Wattmeter	0–10 kW	±0.1%

In the heat source circuit, the temperature of the oil is measured at the inlet and outlet of the evaporator using type-K thermocouples and a high temperature volume flow meter is used to measure the oil flow rate.

The turbine electrical power is measured by means of a 3-phases wattmeter. The characteristics of the measurement devices are reported in Table 2.

2.4. Working fluid selection

Different studies focus on the characteristics required by the fluid in order to retrieve the highest efficiency or power out of the given thermal energy source [8,13]. For low quality waste heat recovery, the choice of the working fluid is often restricted to the refrigerant fluid family because of their low critical temperatures and pressures. However, the availability on trucks of high temperature heat sources such as the recirculated gases (EGR) could also lead to the use of ethanol or water as working fluid.

In the present study, the turbine was designed to operate with R245fa. This fluid is not toxic and not flammable. It is easily available on the market and has null Ozone Depletion Potential (ODP). However it is also characterized by a medium Global Warming Potential (GWP = 1030) and should therefore gradually be removed from the market. Therefore, in addition to an experimental campaign with R245fa, another campaign is then realized with a probable replacement for R245fa: R1233zd (GWP = 6).

2.5. Experimental investigation

Sixty-six, thirty-three with each fluid, of the performed measurement points are used for the comparisons of the two fluids. These points are obtained by keeping the system at a stable condition for a minimum of 15 min and by averaging the measurements over a period of 2 min. The condenser pressure is varied between 2.5 and 4.5 bar absolute for R245fa and between 3 and 4 bar absolute for R1233zd, by step of 0.5 bar, modifying the mass flow rate of the cooling water. The turbine mass flow rate is regulated between 0.15 and 0.35 kg/s by varying the pump rotational speed. For given heat source temperature and mass flow rate, the evaporating pressure is then imposed by the turbine. The rotational speed of the turbine is varied (from 50,000 to 70,000 rpm), as well as the bearings lubrication flow rate (from 0.04 to 0.1 kg/s) which is responsible of internal losses in the bearings.

Given the same heat source and sink conditions (in terms of temperatures at the inlet of the heat exchangers and of mass flow rates), a first comparison is performed operating the two fluids at the same evaporating and condensing temperatures. This enables an objective comparison of the two fluids used in a single system when the evaporating and condensing temperature are limiting the maximum performance of the system because of the heat source and heat sink conditions. Twenty experimental points are used for this comparison, ten with each fluid.

A second method consists in comparing the performance of the system for same condensing temperature levels and same evaporating pressure levels. This enables a comparison adapted to the WHR on truck application where the goal is generally to minimize the condensing pressure, but keeping it above the atmospheric pressure to avoid air infiltration. On the other hand, if the evaporating temperature is not limited by the heat source conditions, which is often the case because of the high temperature of the exhaust gases compared to the critical pressure of the organic fluids, the evaporating pressure can then be optimized to maximize the ORC system performance. Twenty-two experimental points are studied for this comparison, eleven with each fluid.

Please cite this article in press as: Guillaume L et al. Performance of a radial-inflow turbine integrated in an ORC system and designed for a WHR on truck application: An experimental comparison between R245fa and R1233zd. Appl Energy (2016), http://dx.doi.org/10.1016/j.apenergy.2016.03.012

Finally it is proposed to compare both fluids for the same low and high pressure levels to investigate the impact of the fluid on the turbine performance in terms of power output, isentropic efficiency, mass flow rate, rotational speed and lubrication mass flow rate. Twenty-four experimental points were performed for this comparison, twelve with each fluid.

3. Theory/calculation

Firstly the energy balance over the system components is investigated, to cross-check the precision and the quality of the measurements. This step, although often overlooked, is of primary importance because of the numerous measurement issues that can arise in experimental campaigns.

Then the three mass flow rates required to investigate the turbine performance are detailed and the reduced (or corrected) mass flow rate, which will be useful in the comparisons of the turbine performance proposed in this study for the two fluids, is defined.

Finally, the efficiencies of the rotating machines and of the ORC system are defined in order to compare, for both fluids, the performance achieved according to the different test conditions.

3.1. Thermal energy balance

Possible unbalances can indicate measurement errors or unconsidered parasitic phenomena such as ambient losses. The energy balance over the components is calculated as follow:

$$\dot{Q}_{amb} + Er + \dot{W}_{sh} = \dot{m}_{sf} \cdot c_{psf} \cdot (T_{sf,I} - T_{sf,II}) - \dot{m} \cdot (h_{wf,II} - h_{wf,I}) \quad (1)$$

where h_{I}, T_{I} and h_{II}, T_{II} are the inlet (I) and the outlet (II) enthalpy and temperature values of both the working fluid (wf) and the secondary fluid (sf). Specific enthalpies are computed using the open-source CoolProp library [26]. $\dot{m}_{sf}$ and $c_{p,sf}$ are the mass flow and the specific heat capacity of the secondary fluid while $\dot{m}$ is the working fluid mass flow rate. $\dot{Q}_{amb}$ corresponds to the heat ambient losses of the component, Er is the measurement error and $\dot{W}_{sh}$ is the shaft power supplied or consumed by the component.

3.2. Mass flow rates

The flow sent by the pump is split in three parallel flows: the main flow which is expanded in the turbine ($\dot{m}_{tur}$), the flow required for the lubrication of the bearings ($\dot{m}_{lub}$) and the flow required for the cooling of the generator ($\dot{m}_{gen}$). These mass flow rates are measured using Coriolis flow meters and the total mass flow rate can therefore be computed as follow:

$$\dot{m} = \dot{m}_{tur} + \dot{m}_{lub} + \dot{m}_{gen} \quad (2)$$

This total mass flow rate is considered in the definitions of the efficiency of both the pump and the turbine. These components are studied here as systems or black boxes for which all the losses are taken into account. It means, for the pump system: the frequency drive, electrical motor and pump losses. And it means, for the expansion machine system: the turbine, bearings and generator losses.

3.3. Reduced mass flow rate

The reduced mass flow rate of the turbine is defined as follow:

$$\dot{M}^{co} = \frac{\dot{M}_{tur} \cdot \sqrt{T_{wf,ex,tur}}}{P_{wf,ex,tur}} \quad (3)$$

3.4. Pump efficiency

The pump performance was evaluated in a dedicated study. For the needs of the current comparison, a semi-empirical model of the pump, taking into account the leakage and the mechanical losses is used. So the power consumption of the pump, according to the pressure difference between the inlet and outlet and to the mass flow rate, can be calculated using the following isentropic and volumetric efficiency definitions:

$$\varepsilon_{s,pp} = \frac{\dot{W}_{wf,s,pp}}{\dot{W}_{el,pp}} = \frac{\dot{m} \cdot (h_{wf,ex,s,pp} - h_{wf,su,pp})}{\dot{W}_{el,pp}} \quad (4)$$

$$\varepsilon_{v,pp} = \frac{\dot{m}}{\rho_{wf,su} \cdot N_{rot,pp} \cdot V_{s,pp}} \quad (5)$$

3.5. Efficiency of the turbine-generator set

In a first approach, a global efficiency of the turbine-generator set is used to characterize the performance of the component. It is defined through Eq. (6). Then, in order to investigate the potential of improvement of the set, the efficiency of each of the three main components constituting the set (i.e., the turbine, the bearings system and the generator), as depicted in Fig. 14, is defined.

$$\varepsilon_{overall} = \frac{\dot{W}_{el,tur}}{\dot{W}_{wf,s,tur}} = \frac{\dot{W}_{el,tur}}{\dot{m}_{tur} \cdot (h_{wf,su,tur} - h_{wf,ex,s,tur})} \quad (6)$$

The geometry of the turbine being unknown, it is proposed to use the static-to-static definition (7) of the isentropic efficiency of the turbine instead of the total-to-static definition that should be used for a single stage turbine.

$$\varepsilon_{tur,is} = \frac{\dot{W}_{sh}}{\dot{m}_{tur} \cdot (h_{wf,su,tur} - h_{wf,ex,s,tur})} \quad (7)$$

The enthalpy increase of the working fluid from the inlet to the outlet of the bearings system can be evaluated based on the measurements. This enthalpy increase is the result of internal losses in the bearings due to frictions and to the injection of liquid but is also the consequence of a heat transfer by convection between the fluid expanded in the turbine and the fluid lubricating the bearings. Considering these phenomena indivisible in the scope of this paper, the bearing efficiency is defined as follow:

$$\varepsilon_{lub} = \frac{\dot{W}_{sh} - \dot{m}_{lub} \cdot (h_{wf,ex,lub} - h_{wf,su,lub})}{\dot{W}_{sh}} \quad (8)$$

In the same way, the enthalpy increase of the working fluid from the inlet to the outlet of the generator can be evaluated and the efficiency of the generator can be calculated.

$$\varepsilon_{gen} = \frac{\dot{W}_{el,tur}}{\dot{W}_{sh} - \dot{m}_{lub} \cdot (h_{wf,ex,lub} - h_{wf,su,lub})} \quad (9)$$

Finally, these three efficiencies can be linked to the global efficiency (6) through Eq. (10).

$$\varepsilon_{overall} = \varepsilon_{tur,is} \cdot \varepsilon_{lub} \cdot \varepsilon_{gen} \quad (10)$$

3.6. Cycle efficiency

The cycle efficiency is calculated based on the first law of thermodynamics.

$$\eta_{cycle} = \frac{\dot{W}_{el,tur} - \dot{W}_{el,pp}}{\dot{Q}_{ev}} \quad (11)$$

Please cite this article in press as: Guillaume L et al. Performance of a radial-inflow turbine integrated in an ORC system and designed for a WHR on truck application: An experimental comparison between R245fa and R1233zd. Appl Energy (2016), http://dx.doi.org/10.1016/j.apenergy.2016.03.012

4. Results and discussion

4.1. Thermal energy balances

Thermal energy balances over the evaporator, the condenser and the turbine for both R245fa and R1233zd are expressed for the sixty-six measurements points. An uncertainty propagation study is performed and results are shown and explained in Appendix A.

4.2. Link between mass flow rate, reduced mass flow rate and pressure ratio

Expressing the mass flow rate of the turbine as a function of the pressure ratio leads, for the sixty-six measurement points, to Fig. 3. In this figure, linear relations between the mass flow rate and the pressure ratio can be deduced for each fluid (three and two relations for R245fa and R1233zd respectively). Each straight correspond to one of the investigated condensing pressures for each fluid. This means that, in fact, the mass flow rate of the turbine depends only on the turbine inlet pressure. This is why, among other, the two linear relations obtained with R1233zd are confounded with two of those obtained with R245fa. They correspond to same condensing pressure levels in addition to the fact that the fluids have very similar thermophysical properties.

The use of the reduced mass flow rate should be preferred. Thus, a single linear relation now fits the evolution of the reduced mass flow rate as a function of the pressure ratio presented in Fig. 4. As it can be observed, this relation is valid for both fluids and the different investigated condensing pressure levels.

4.3. Performance comparison for same temperature levels

A thermodynamic comparison of both working fluids for same condensing and evaporating temperature levels is certainly the most objective comparison. It enables to compare the performance of a single system, using the two fluids, in the case of same heat source and heat sink conditions.

In practice, the objective function of a WHRORC is generally to maximize the power output of the system [13]. From the Definition (6), it can be deduced that maximizing the power output of the expansion machine is achieved by optimizing the pressure ratio, the inlet temperature (TIT), the rotational speed and the mass flow rate of the expansion machine. These magnitudes are linked together and, aside from the temperature and the rotational speed, in the case of the studied radial turbine, the relation between the pressure ratio and the mass flow rate is linear (Figs. 3 and 4). Maximizing the output power of the turbine is therefore achieved by maximizing the pressure ratio (and therefore the mass flow rate) inside the design operating range of [2–5].

However, the maximal evaporating pressure and the minimal condensing pressure are, for given heat source and heat sink conditions, limited by the efficiency of the heat exchangers. There is

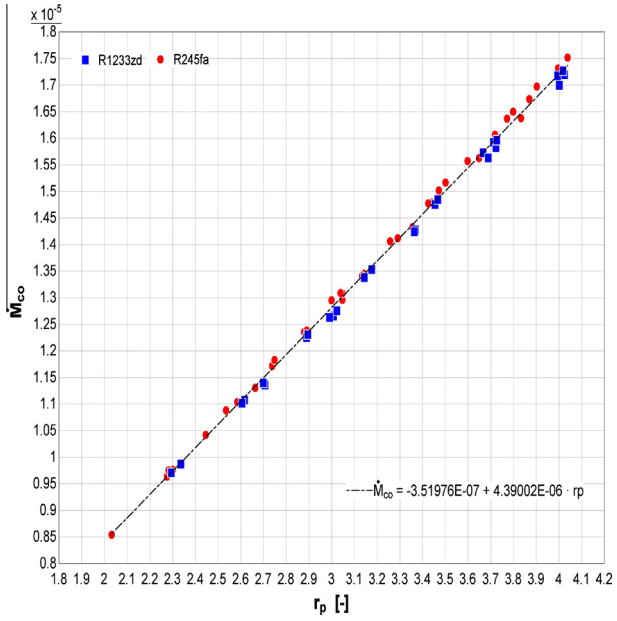

Fig. 4. Evolution of the reduced mass flow rate as a function of the pressure ratio for both fluids.

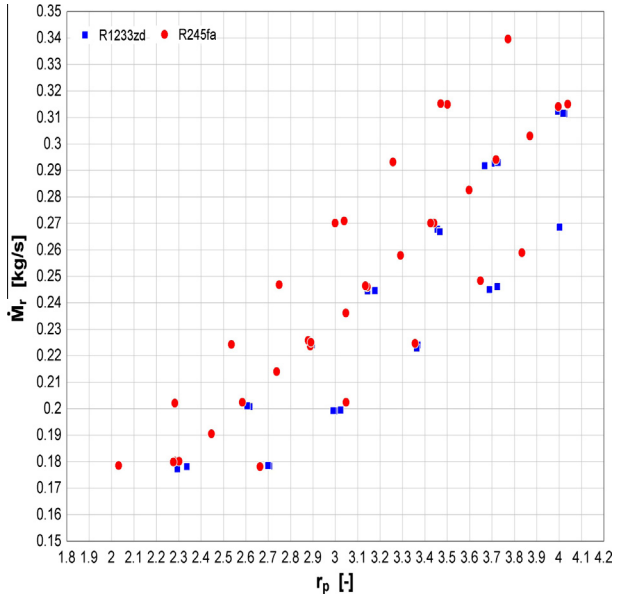

Fig. 3. Evolution of the mass flow rate as a function of the pressure ratio for both fluids.

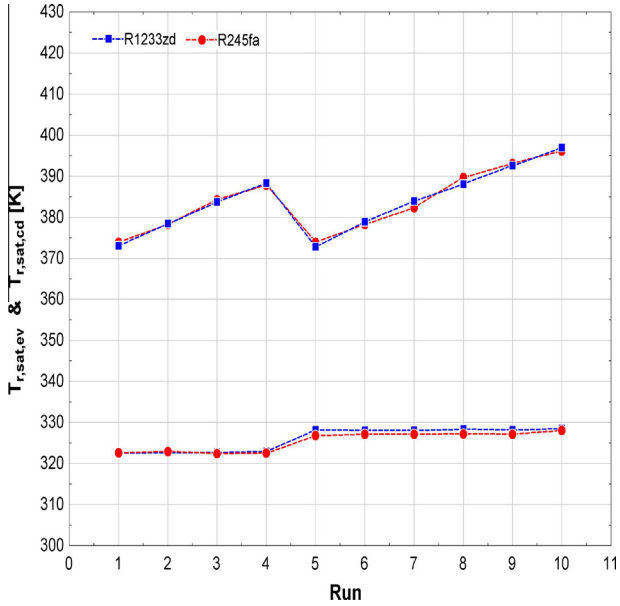

Fig. 5. Comparison between evaporating and condensing temperature levels for both fluids.

Please cite this article in press as: Guillaume L et al. Performance of a radial-inflow turbine integrated in an ORC system and designed for a WHR on truck application: An experimental comparison between R245fa and R1233zd. Appl Energy (2016), http://dx.doi.org/10.1016/j.apenergy.2016.03.012

a minimum temperature difference between the secondary and the primary fluids that can be reached in the heat exchangers. In other words, for given heat source and heat sink conditions, the pressure ratio of the cycle is limited by the maximal evaporating temperature and minimal condensing temperature that can be achieved. This justify therefore this first comparison.

Looking at the fluid properties, overall, the pressure level corresponding to the same saturation temperature is lower using R1233zd than using R245fa. As it can be seen based on the 20 measurements point in Figs. 5 and 6, this phenomenon is growing with temperature. Both the condensing pressure and evaporating pressure are therefore reduced when using R1233zd but the latter pressure is much more affected.

It thus results in a lower pressure ratio and, as it as been showed previously (Fig. 3), in a lower mass flow rate. The turbine power production (evaluated for same rotational speed and lubricating flow rate) is therefore lower using R1233zd than using R245fa. However the pump consumption is also reduced. At the end, the net output power of the system remains comparable for both fluids as it can be seen in Fig. 7 showing the evolution of the turbine power output and of the ORC net power output as functions of the pressure ratio.

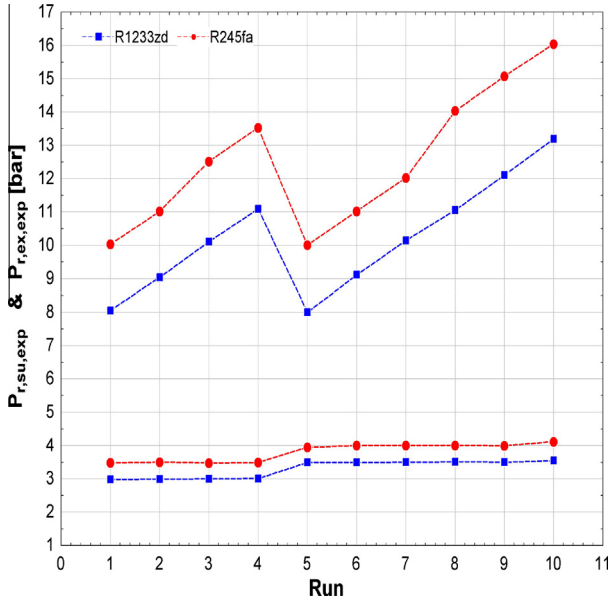

Fig. 6. Comparison between evaporating and condensing pressure levels for both fluids.

4.4. Performance comparison for optimized pressure levels

In the case of a WHRORC system for truck application, one of the main target is to reach a condensing pressure as low as possible (but above the atmospheric pressure to avoid air infiltration). A fluid whose pressure level is lower for the same saturation temperature, everything else remaining equal, will then be preferred.

On the other hand, the evaporating pressure can be optimized to maximize the power output of the ORC system according to the exhaust gases temperature and mass flow rate conditions. As explained in the previous section, the evaporating pressure is generally limited by the maximal evaporating temperature that can be reached according to the heat source conditions. However, because of the high temperature of the exhaust gases compared to the evaporating temperature of R245fa or R1233zd, when used in subcritical ORC systems, and if the exhaust gases mass flow rate is sufficient, the limit on the evaporating pressure is no longer the temperature but the limit permitted in the framework of the application. This limit depends among other of the material that are used and is provided by standards.

That is why in this section, both fluids are compared for same condensing temperature levels (Fig. 8) and same evaporating pressure levels (Fig. 9) for 22 additional measurements points. It is therefore assumed that the evaporating temperature of the working fluid can be increased, when passing from R245fa to R1233zd, for the same exhaust gases conditions. A T–s diagram of the cycle can be found in Fig. 19 of Appendix B where the evaporating pressure is 11 barA for both fluids and the condensing pressure is 3 barA for R1233zd and 3.5 barA for R245fa. Results are compared in terms of working fluid mass flow rate, pump power consumption and turbine power production.

The conditions of this comparison (same evaporating pressure) lead to the same mass flow rates for both fluids. Nonetheless, the pump power consumption is slightly lower when using R1233zd. This is explained by lower pressure drops between the pump and

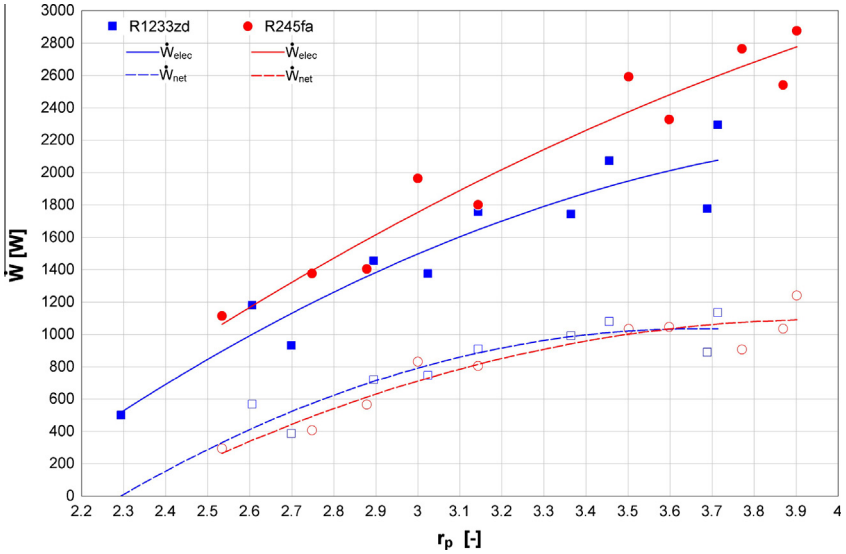

Fig. 7. Comparison between the turbine power production and the system net output power for both fluids.

Please cite this article in press as: Guillaume L et al. Performance of a radial-inflow turbine integrated in an ORC system and designed for a WHR on truck application: An experimental comparison between R245fa and R1233zd. Appl Energy (2016), http://dx.doi.org/10.1016/j.apenergy.2016.03.012

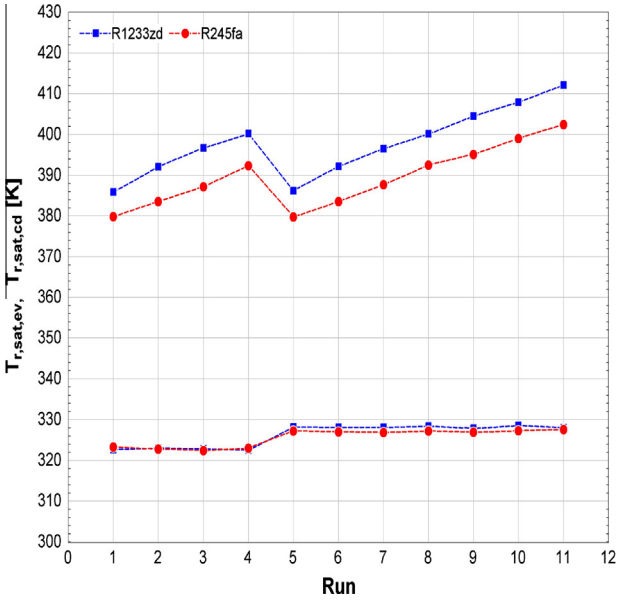

Fig. 8. Comparison between evaporating and condensing temperature levels for both fluids.

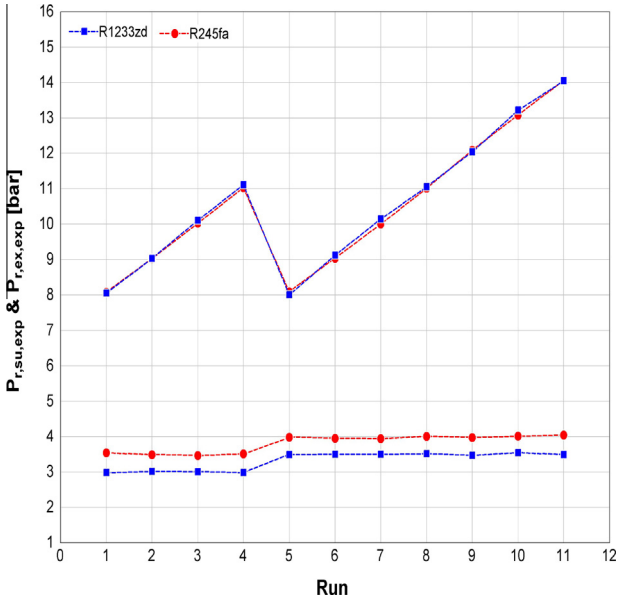

Fig. 9. Comparison between evaporating and condensing pressure levels for both fluids.

the turbine. The pressure at the pump outlet is therefore lower when using R1233zd.

In Fig. 10, the power produced by the turbine is compared for both fluids and for same rotational speeds and same lubrication mass flow rates. As it could be expected, the power produced is always higher using R1233zd. Because of the comparison method, the pressure ratio over the turbine is in each case higher than for R245fa. Since the mass flow rates are the same, the power produced is increased when using R1233zd. A lower pump consumption and a higher turbine power production using R1233zd, obviously leads to a larger net output power of the system that can be increased by 40%.

4.5. Performance comparison for same pressure levels

In order to investigate the impact of the working fluid on the turbine performance, a last comparison, involving 24 new measurements points and for same evaporating and condensing pressure levels is performed. A T–s diagram of the cycle can be found in Fig. 20 of Appendix B where the evaporating pressure is 14 barA and the condensing pressure is 3.5 for both fluids.

The evaporating pressure being the same, the mass flow rates are the same for both fluids. The pump consumption remains slightly lower when using R1233zd because of lower pressure drops between the pump and the turbine. Regarding the turbine, in this case, the maximal power achieved with the two fluids for each pressure levels is compared. Thus, in this comparison, the rotational speed and the lubrication flow rate are no more the same for each fluid but both the variables are optimized.

As it can be seen in Fig. 12, even for the same pressure ratio and the same mass flow rate, the power production is slightly higher using R1233zd. This can be explained by a lower lubrication flow rate and/or a higher rotational speed closer of the turbine optimal speed with this fluid.

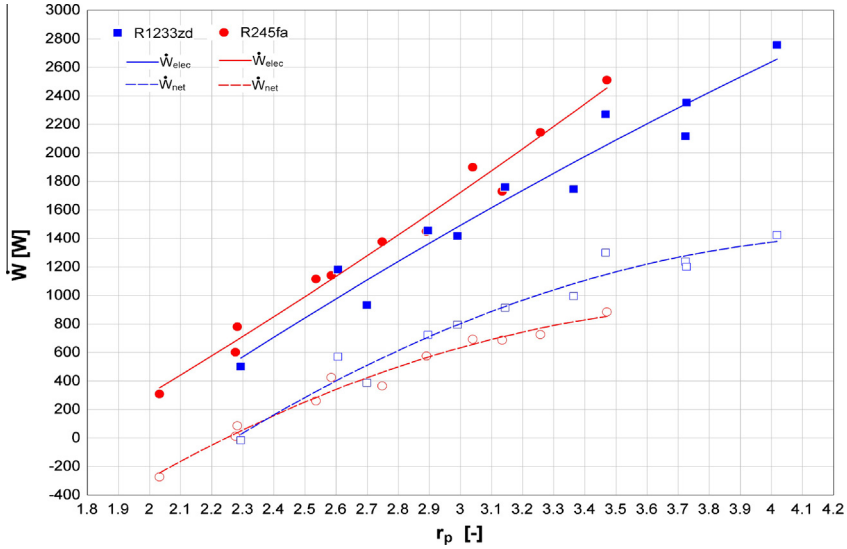

Fig. 10. Comparison between the turbine power production and the system net output power for both fluids.

Please cite this article in press as: Guillaume L et al. Performance of a radial-inflow turbine integrated in an ORC system and designed for a WHR on truck application: An experimental comparison between R245fa and R1233zd. Appl Energy (2016), http://dx.doi.org/10.1016/j.apenergy.2016.03.012

Indeed, for a given lubrication flow rate, an increase in rotational speed corresponds to an increase in the temperature of the bearings and of the lubricant because of higher mechanical losses. A maximal rotational speed can then be defined just before reaching the maximal temperature allowed in this location. Therefore the optimal speed leading to the best turbine efficiency cannot always be reached if this speed is higher than the maximal speed allowed by the bearings system.

On the other hand, the lubrication flow rate is adjusted to ensure the fluid leaving the bearings system is in liquid phase. Otherwise the bearings would risk to run dry and to be quickly broken. However this lubrication flow rate is responsible of additional pump consumption but also of internal losses in the bearings system that consume part of the power produced by the turbine. To achieve the minimum pump consumption and the best turbine-generator overall efficiency (Fig. 13), the lubrication mass flow rate has therefore to be reduced to a minimum but must remain sufficient to guarantee a degree of subcooling at the outlet of the bearings system. A level of subcooling around 5 K, before reaching the saturation temperature at the corresponding condensing pressure, was kept as a safety limit.

Because the saturation temperature for a same pressure level is around 5 K higher when using R1233zd compared to R245fa, the speed could be increased and/or the lubrication flow rate could be reduced in a bigger proportion as shown in Fig. 11. This explains the better performance of the turbine, in terms of power produced (Fig. 12) and isentropic efficiency (Fig. 13), when using R1233zd. In this latter Figure, the impact of the lubrication flow rate and of the rotational speed on the turbine efficiency can be particularly well observed for the third measurement point for which the differences between the two fluids are the most important.

In addition, the difference of saturation temperature between the fluids also enables to reach higher evaporating pressures and therefore pressure ratios using R1233zd before meeting the temperature limit at the outlet of the bearings system. Thus, for instance, in the case where the condensing pressure is 3 bar

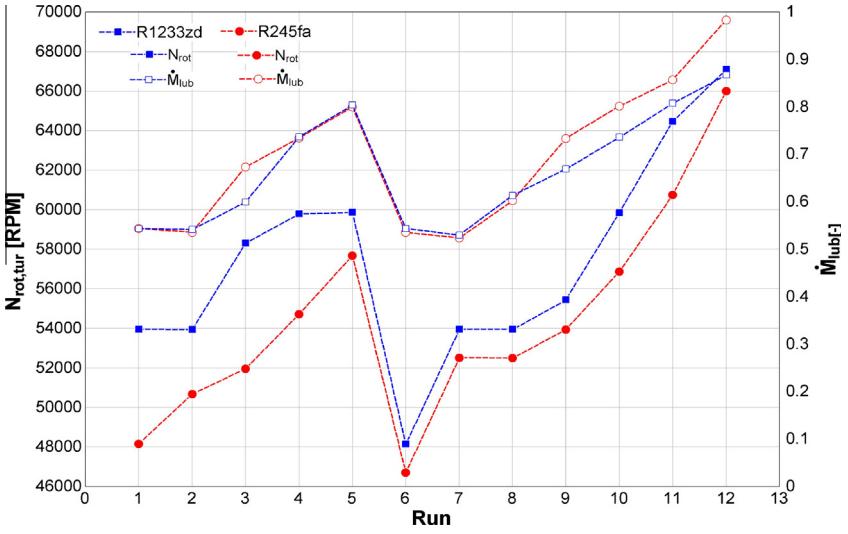

Fig. 11. Comparison between the turbine rotational speed and the lubrication flow rate for both fluids.

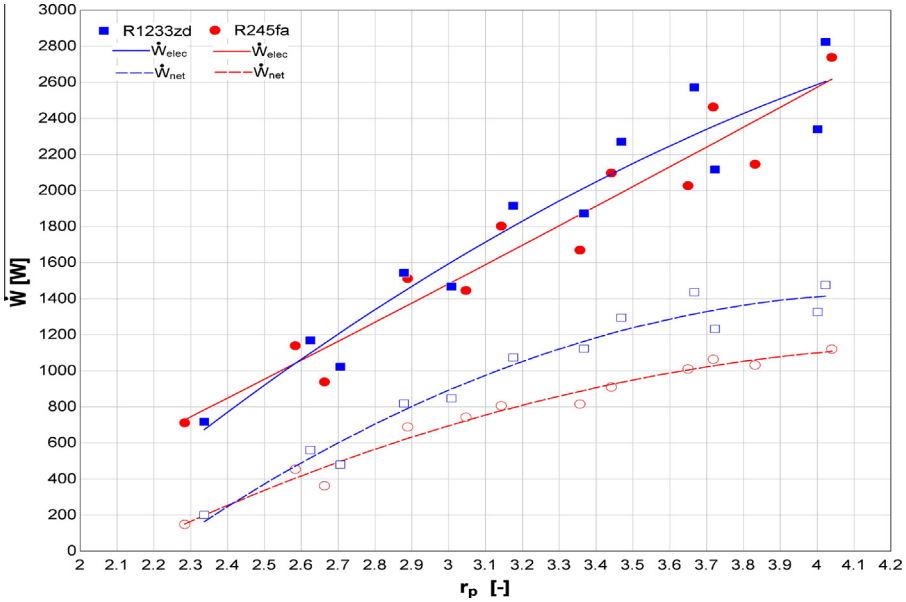

Fig. 12. Comparison between the turbine power production and the system net output power for both fluids.

Please cite this article in press as: Guillaume L et al. Performance of a radial-inflow turbine integrated in an ORC system and designed for a WHR on truck application: An experimental comparison between R245fa and R1233zd. Appl Energy (2016), http://dx.doi.org/10.1016/j.apenergy.2016.03.012

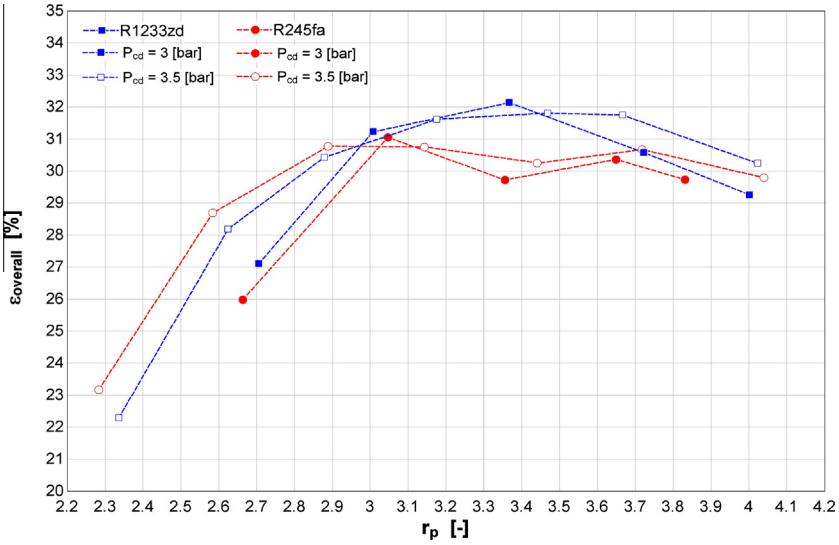

Fig. 13. Comparison between the turbine isentropic efficiency as a function of the pressure ratio for both condensing pressure levels and both fluids.

absolute, a maximal evaporating pressure of 12 bar can be reached using R1233zd while it is limited to 11.5 bar absolute with R245fa.

4.6. Potential of improvement

In average over the 66 measurement points, the global efficiency of the turbine-generator set is around 28%. Consequently there seems to be a large potential of improvement regarding this first prototype, which is initially devoted to be integrated in an on board WHR system.

Combining this performance with the efficiency of the pump system varying between 29% and 42%, this leads to a cycle efficiency reaching 1.8%. However, the pump system efficiency takes into account the losses of the frequency drive and of the electric motor, which is the weakness of the overall effectiveness (more details on the efficiency and the losses distribution of pump systems can be found in [27]). Therefore, the pump system considered in this study could not be integrated in the on board WHR system. Indeed, in addition to its low efficiency at part load, the electric motor is simply to heavy. The latter should be replaced or a mechanical coupling between the pump and the shaft the truck engine could be envisaged. Nonetheless, even if a mechanical efficiency of 90% could be achieved, thus rising the pump system efficiency up to 89%, the ORC efficiency would only reach 2.5%. Accordingly, the effort to increase the cycle efficiency should be place on the turbine-generator set.

The pump put aside, increasing the global efficiency of the turbine-generator set requires initially to identify and dissociate the different sources of losses of the system.

First the system can be seen as a combination of three subsystems that are the turbine, the bearings system and the generator (Fig. 14). Thus the previously defined overall turbine efficiency (6) can be split into:

- the turbine static-to-static efficiency (7),
- the efficiency of the bearings system (8),
- the conversion efficiency of the generator (9).

These efficiencies can be evaluated (and linked to the overall turbine efficiency (10)) based on the first law of thermodynamics.

Indeed, the temperature, pressure and mass flow rate of working fluid are measured at the inlet and outlet of each of the three subsystems. Starting from the electrical power produced by the generator, the conversion efficiency of the generator can be evaluated assuming that all the losses taking place in this subsystem are dissipated in heat which is entirely transferred to the cooling fluid.

In the same way, the efficiency of the bearings system can be then evaluated. The internal losses of the bearings system are assumed to be dissipated in heat which is transferred entirely to the lubricant. In addition, the heat exchanged by convection from the fluid expanded in the turbine to the bearings lubricant has to be taken into account. This heat transfer is assumed not affecting

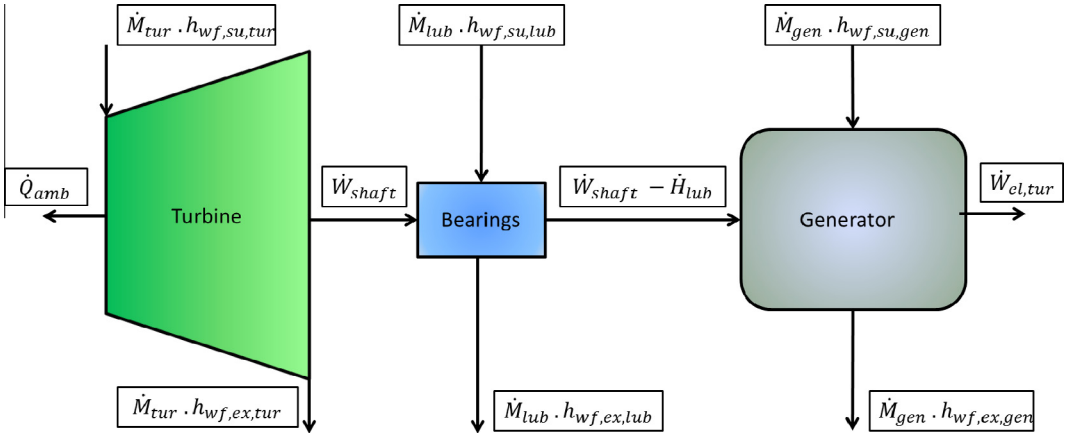

Fig. 14. Schematics of the three subsystems constituting the turbine-generator set.

Please cite this article in press as: Guillaume L et al. Performance of a radial-inflow turbine integrated in an ORC system and designed for a WHR on truck application: An experimental comparison between R245fa and R1233zd. Appl Energy (2016), http://dx.doi.org/10.1016/j.apenergy.2016.03.012

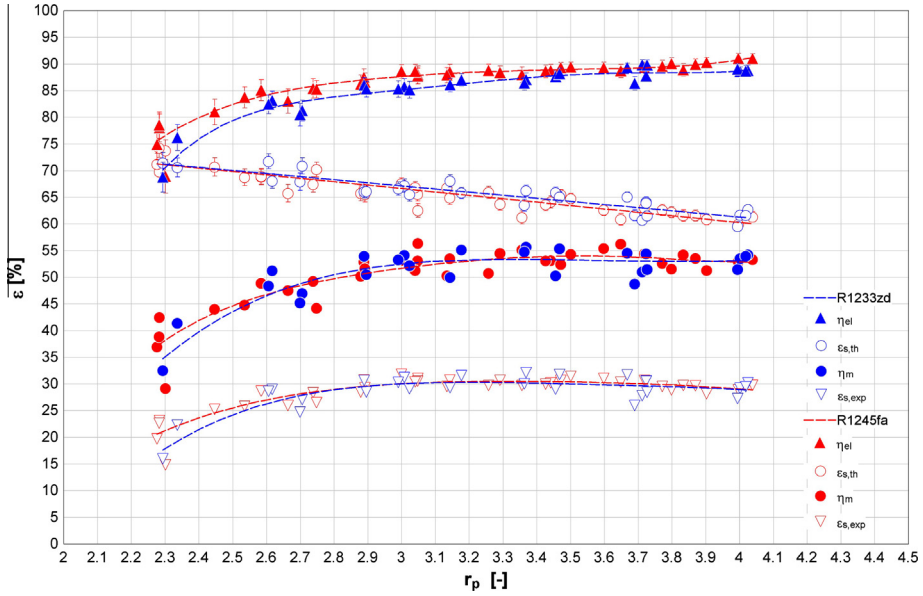

Fig. 15. Evolution of the turbine isentropic efficiency, bearings system efficiency, generator efficiency and overall system efficiency as functions of the pressure ratio for both working fluid.

the intrinsic aerodynamic quality of the flow in the turbine and, in the scope of this paper, remains indivisible with the heat resulting from internal losses of the bearings.

Finally, the static-to-static isentropic efficiency of the turbine can be evaluated.

The evolution of the turbine isentropic efficiency, of the bearings system efficiency, of the generator efficiency and of the overall system efficiency as functions of the pressure ratio for both working fluid and for the 66 measurements points is presented in Fig. 15. Several observations can be performed:

- Firstly, the value of the efficiencies does not seem affected by the choice of the working fluid. Similar values are obtained with both fluids.
- Secondly, as it could be expected, the generator efficiency is increasing with the mechanical power and therefore with the turbine pressure ratio. The range of variation of this efficiency is in between 70% and 90%.
- Thirdly, the turbine isentropic efficiency is decreasing almost linearly with the pressure ratio. However the efficiency remains acceptable over the large range of pressure conditions since it is ranging from 75% to 60%. This behavior of the efficiency of the radial inflow technology, also pointed out in [13], added to the absence of oil are important advantages compared to other expansion machines.
- Fourthly the efficiency of the bearing system is relatively low, ranging from 29% to 56%. This indicates that the priority, in order to increase the overall efficiency of the turbine-generator set, should be placed on the improvement of the bearings system and of its lubrication.

The increase of the bearings system efficiency with the pressure ratio indicates that internal losses are probably the main source of losses compared to the convective heat transfer from the expanded fluid to the lubricant. Indeed, increasing the pressure ratio implies to increase the turbine inlet pressure and therefore, keeping a constant overheating, to increase the TIT. This means that, if the heat loss due to the heat transfer was predominant, the efficiency of the bearings system should decrease with the pressure ratio.

As for the pump system, if the mechanical efficiency of the turbine-generator set could hypothetically reach 90%, this would rise the system overall efficiency from 28% to 51% and the ORC efficiency up to 4.8%. At this stage, the generator, limiting the electrical power to 3.5 kWe, should be replaced since the produced power could rise, everything else remaining equal, up to 5.3 kWe.

To go further the turbine itself should then be investigated more into details. All the sources of losses (leakages, windage losses, incidence losses, friction losses, etc.) taking place in this component could be identified and quantified in order to point out the opportunities for improvement in the design of the turbine. Nonetheless, such an investigation will require to develop a relatively detailed model of the turbine and is out of the scope of this study.

5. Conclusion

Small scale ORC systems can play a key role for low grade waste heat recovery applications. In this work an experimental campaign is achieved to compare the performance of an WHRORC system equipped with a radial-inflow turbine for two working fluids: R245fa and its probable substitute R1233zd.

The evaporator, the condenser and the turbine performance is checked by analyzing the thermal energy balance over each of them and an uncertainty propagation study is performed. This step is of primary importance because of the numerous measurement issues that can arise in experimental campaigns.

Three types of comparison are then proposed for the performance of the ORC components. A first comparison based on same temperature levels for both fluids is performed. This is an objective comparison that enables to compare the performance of the same system for same heat source and heat sink conditions. Because the saturation temperature is higher with R1233zd than R245fa for a same pressure level and because this phenomenon is growing with the temperature level, the pressure ratio and therefore the mass flow rate are lower with R1233zd. This leads to a lower turbine power output but also to a lower pump consumption. At the end, comparable net output power are observed using both fluids.

Secondly the performance is compared for same condensing temperatures and same evaporating pressures. Indeed, for the truck application, one of the main target is to reach a condensing pressure as low as possible. A fluid with a lower condensing pressure for a same saturation temperature level, everything else

Please cite this article in press as: Guillaume L et al. Performance of a radial-inflow turbine integrated in an ORC system and designed for a WHR on truck application: An experimental comparison between R245fa and R1233zd. Appl Energy (2016), http://dx.doi.org/10.1016/j.apenergy.2016.03.012

remaining equal, is suited. On the other hand, the evaporating pressure can be optimized if the exhaust gases temperature and mass flow rate conditions are not limiting the evaporating temperature. Results showed that the pressure conditions used for the comparison led to the same mass flow rates for both fluids. Nonetheless, the pump consumption is slightly lower in case of R1233zd. The power produced by the turbine is always higher when using R1233zd because of the higher pressure ratio resulting of the comparison method.

Finally, the performance is compared for same pressure levels. This comparison is convenient to investigate the impact of the working fluid on the turbine performance, the pressure ratio being the same. The turbine being lubricated by the fluid, better results are achieved when using R1233zd compared to R245fa. Indeed, for same pressure levels and mass flow rates, R1233zd enables the turbine to be operated at higher speed and/or with a lower lubrication flow rate which is also a source of losses.

This analysis experimentally demonstrates that, based on the given test-rig, R1233zd represents a better choice compared to R245fa to recover the waste heat of the exhaust gases of a long haul truck.

However there is a large potential of improvement regarding the turbine-generator set. The overall efficiency, indeed, averaged over the 66 measurements points, is around 28%. Improving this efficiency requires to identify and quantify the different sources of losses so to reduce them. First the defined global turbine efficiency can be split in:

- the turbine static-to-static efficiency,
- the efficiency of the bearing system,
- the efficiency of the generator.

This separation is possible based on the first law of thermodynamics and using the temperature, pressure and mass flow rate measurements performed on the working fluid at the inlet and outlet of each subsystem. A static-to-static isentropic efficiency varying between 60% and 75% is identified for the turbine and a range from 70% to 90% is identified for the generator efficiency. The efficiency of the bearing system is relatively low, ranging from 29% to 56%. This low efficiency, taking into account the internal losses due to frictions in the bearings system and liquid injection but also the heat transferred by convection from the fluid expanded in the turbine to the fluid lubricating the bearings, indicates that the priority, in order to increase the overall efficiency of the turbine-generator set, should be placed on the improvements of the bearings system and its lubrication.

Finally the turbine itself should be investigated more into details. All the sources of losses (leakages, windage losses, incidence losses, friction losses, incidence losses, etc.) taking place in this component could be identified and quantified in order to point out the opportunities for improvement in the design of the turbine.

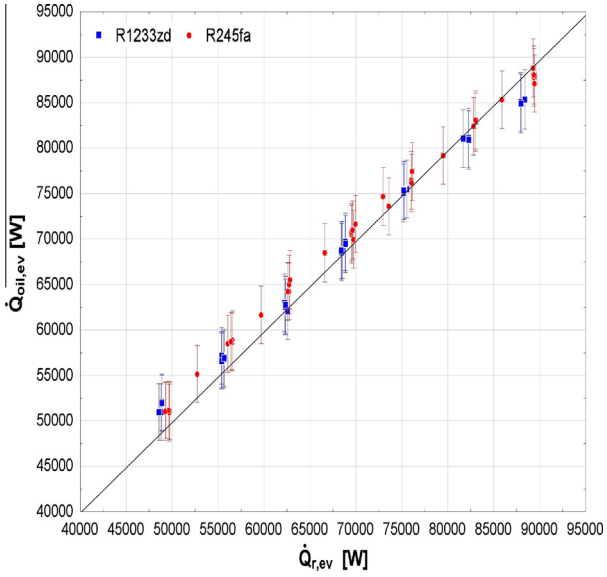

Fig. 16. Heat balance over the evaporator.

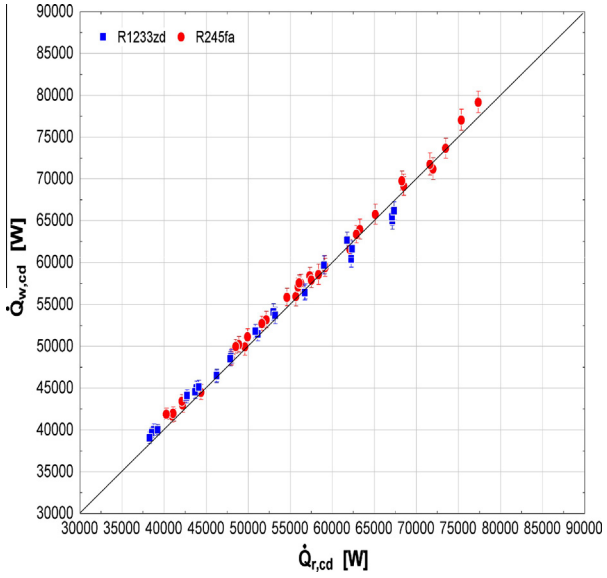

Fig. 17. Heat balance over the condenser.

Appendix A. Thermal energy balances

A.1. Heat exchangers

Both exchangers being insulated, the difference between the corresponding heat flow rates on the secondary and the primary fluid sides is practically null (Figs. 16 and 17). The maximal difference is around 6% regarding the evaporator and 3% regarding the condenser. As it can be seen through the uncertainty bars on Figs. 16 and 17, this can be explained by the measurement accuracy of the sensors. However the ambient losses also justify the difference between the corresponding heat flow rates on the primary and secondary fluid side for both heat exchangers and particularly the evaporator.

A.2. Turbine

The energy balance over the turbine can be expressed as follow:

$$\dot{H}_{tur} + \dot{H}_{lub} + \dot{H}_{gen} = \dot{Q}_{amb} + \dot{W}_{elec} \quad (12)$$

where

$\dot{H}_{tur} = \dot{M}_{tur}.(h_{wf,su,tur} - h_{wf,ex,tur})$ is the enthalpy flow rate over the turbine
$\dot{H}_{lub} = \dot{M}_{lub}.(h_{wf,ex,pp} - h_{wf,ex,lub})$ is the enthalpy flow rate over the bearings
$\dot{H}_{gen} = \dot{M}_{gen}.(h_{wf,ex,pp} - h_{wf,ex,gen})$ is the enthalpy flow rate over the generator
$\dot{Q}_{amb}$ are the ambient losses
$\dot{W}_{elec}$ is the electrical power produced by the turbine generator

Please cite this article in press as: Guillaume L et al. Performance of a radial-inflow turbine integrated in an ORC system and designed for a WHR on truck application: An experimental comparison between R245fa and R1233zd. Appl Energy (2016), http://dx.doi.org/10.1016/j.apenergy.2016.03.012

Based on the sensors installed on the rig, the different mass flow rates are known as well as the different temperature and pressure levels at the inlet and outlet of the turbine, the bearings and the generator. The corresponding enthalpy values can therefore be calculated. The electrical power produced being also measured, expressing the energy balance over the turbine result finally in estimating the remaining unknown of the previous equations system, the ambient losses of the turbine. These ambient losses are presented in Fig. 18 as a function of the pressure ratio. On this figure, a part of the mean values of the ambient losses appear to be negative, even if they are close to 0. This is explained by the high sensitivity of the heat balance (12) with respect to the turbine inlet temperature. Indeed, the measurement accuracy (0.5 K) of the type-T thermocouples is enough to explain the uncertainties of ±200 [W] in average on the ambient losses presented on the same figure. Taking this fact into account, the energy balance on the turbine appears therefore correct and the measurements can be trusted.

Another remarkable fact is the spread of the ambient losses when the pressure ratio is increasing. The increase of the ambient losses is obviously linked to the inlet temperature of the turbine, which is, for a given overheating, increasing with the inlet pressure. However, a fixed pressure ratio value, the spread of he ambient losses is explained by different rotational speed and lubrication flow rates. Indeed, a high rotational speed and a low lubrication flow rate lead to higher temperature of the turbine and reversely.

Appendix B. T–s diagrams

See Figs. 19 and 20.

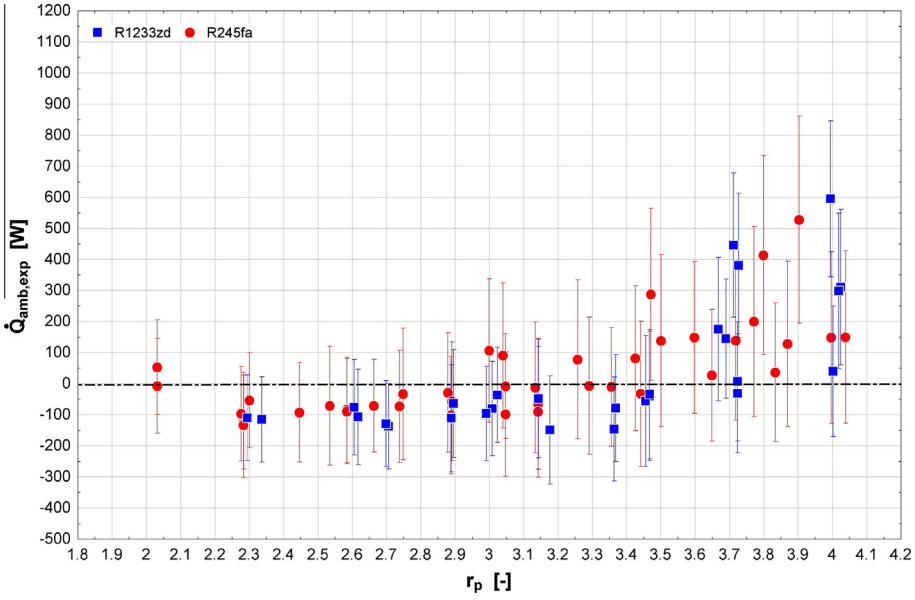

Fig. 18. Resulting ambient heat losses from the energy balance over the turbine.

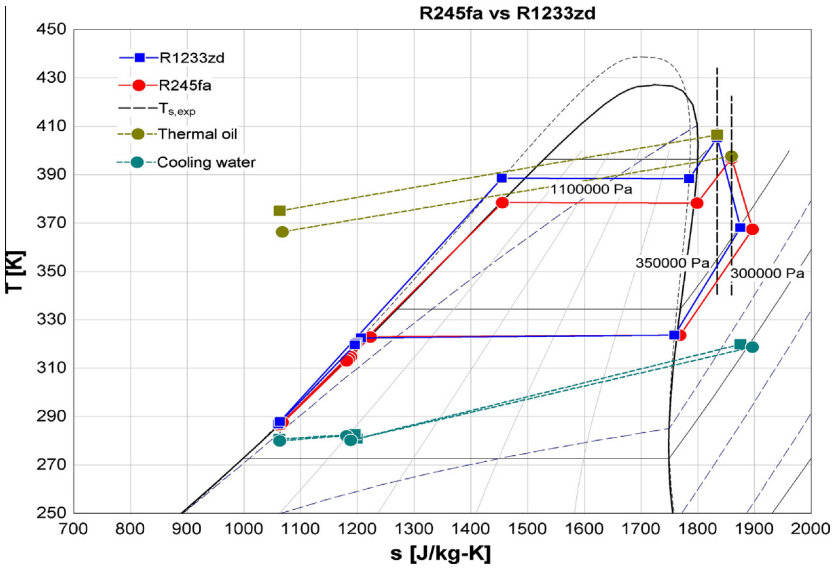

Fig. 19. Performance comparison for optimized pressure levels: T–s diagram of the cycle for both fluids.

Please cite this article in press as: Guillaume L et al. Performance of a radial-inflow turbine integrated in an ORC system and designed for a WHR on truck application: An experimental comparison between R245fa and R1233zd. Appl Energy (2016), http://dx.doi.org/10.1016/j.apenergy.2016.03.012

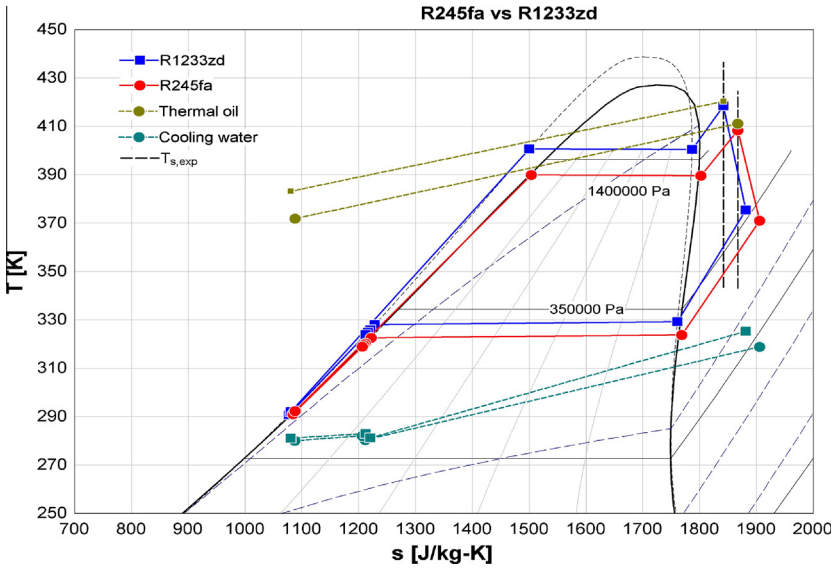

Fig. 20. Performance comparison for same pressure levels: T–s diagram of the cycle for both fluids.

References

[1] Kokic P, Crimp S, Howden M. A probabilistic analysis of human influence on recent record global mean temperature changes. Clim Risk Manage 2014;3:1–12.
[2] IEA, Key world energy statistics; 2014. <http://www.iea.org/publications/freepublications//publication/KeyWorld2014.pdf>.
[3] UNFCCC, Kyoto protocol to the united nations framework convention on climate change; 1992. <http://unfccc.int/resource/docs/convkp/kpeng.html>.
[4] European comission, Climate action. <http://europa.eu/pol/pdf/flipbook/fr/climate_action_fr.pdf>.
[5] European comission, Towards a strategy to address co2 emissions from hdv.; 2013. <http://ec.europa.eu/clima/policies/transport/vehicles/heavy/index.htm>.
[6] Espinosa N, Tilman L, Lemort V, Quoilin S, Lombard B, Rankine cycle for waste heat recovery on commercial trucks: approach, constraints and modelling. In: SIA, diesel international conference and exhibition; 2010.
[7] Badr O, Probert SD, O'Callaghan PW. Selecting a working fluid for a rankine cycle engine. Appl Energy 1985;21:1–42.
[8] Bao J, Zhao L. A review of working fluid and expander selections for organic rankine cycle. Renew Sustain Energy Rev 2013;24:325–42.
[9] Toffolo A, Lazzaretto A, Manente G, Paci M. A multi-criteria approach for the optimal selection of working fluid and design parameters in organic rankine cycle systems. Appl Energy 2014;121:219–32.
[10] Shu G, Liu L, Tian H, Wei H, Yu G. Parametric and working fluid analysis of a dual-loop organic rankine cycle (DORC) used in engine waste heat recovery. Appl Energy 2014;113:1188–98.
[11] Latz G, Andersson S, Munch K, Selecting an expansion machine for vehicle waste-heat recovery systems based on the rankine cycle. SAE Technical Paper 2013-01-0552; 2013. doi:http://dx.doi.org/10.4271/2013-01-0552.
[12] Macián V, Serrano JR, Dolz V, Sánchez J. Methodology to design a bottoming rankine cycle, as a waste energy recovering system in vehicles. study in a HDD engine. Appl Energy 2013;104:758–71.
[13] Quoilin S, Van Den Broek M, Declaye S, Dewallef P, Lemort V. Techno-economic survey of organic rankine cycle (ORC) systems. Renew Sustain Energy Rev 2013;22:168–86.
[14] Zheng N, Zhao L, Wang XD, Tan YT. Experimental verification of a rolling-piston expander that applied for low-temperature organic rankine cycle. Appl Energy 2012;112:1265–74.
[15] Costall AW, Gonzalez Hernandez A, Newton PJ, Martinez-Botas RF. Design methodology for radial turbo expanders in mobile organic rankine cycle applications. Appl Energy 2015;157:729–43.
[16] Song J, Gu CW. Performance analysis of a dual-loop organic rankine cycle (ORC) system with wet steam expansion for engine waste heat recovery. Appl Energy 2015;156:280–9.
[17] Di Battista D, Mauriello M, Cipollone R. Waste heat recovery of an ORC-based power unit in a turbocharged diesel engine propelling a light duty vehicle. Appl Energy 2015;152:109–20.
[18] Arunachalam P, Shen M, Tuner M, Tunestal P, Thern M, Waste heat recovery from multiple heat sources in a HD truck diesel engine using a rankine cycle – a theoretical evaluation. SAE Technical Paper 2012-01-1602; 2012. doi:http://dx.doi.org/10.4271/2012-01-1602.
[19] Yamaguchi T, Aoyagi Y, Uchida N, Fukunaga A, Kobayashi M, Adachi T, et al. Fundamental study of waste heat recovery in the high boosted 6-cylinder heavy duty diesel engine. SAE Int J Mater Manuf 2015;8(2):209–26. http://dx.doi.org/10.4271/2015-01-0326.
[20] Allouache A, Leggett S, Hall M, Tu M, Baker C, Fateh H. Simulation of organic rankine cycle power generation with exhaust heat recovery from a 15 liter diesel engine. SAE Int J Mater Manuf 2015;8(2):227–38. http://dx.doi.org/10.4271/2015-01-0339.
[21] Amicabile S, Leeb JI, Kum D. A comprehensive design methodology of organic rankine cycles for the waste heat recovery of automotive heavy-duty diesel engines. Appl Therm Eng 2015;87:574–85.
[22] Xie H, Yang C. Dynamic behavior of rankine cycle system for waste heat recovery of heavy duty diesel engines under driving cycle. Appl Energy 2013;112:130–41.
[23] Furukawa T, Nakamura M, Machida K, Shimokawa K, A study of the rankine cycle generating system for heavy duty HV trucks. SAE Technical Paper 2014-01-0678; 2014. doi:http://dx.doi.org/10.4271/2014-01-0678.
[24] Park T, Teng H, Hunter G, van der Velde B, Klaver J, A rankine cycle system for recovering waste heat from HD diesel engines – experimental results. SAE Technical Paper 2011-01-1337; 2011. doi:http://dx.doi.org/10.4271/2011-01-1337.
[25] Rahbar K, Mahmoud S, Al-Dadah RK, Moazami N. Modelling and optimization of organic rankine cycle based on a small-scale radial inflow turbine. Energy Convers Manage 2015;91:186–98.
[26] Bell I, Wronski J, Quoilin S, Lemort V. Pure and pseudo-pure fluid thermophysical property evaluation and the open-source thermophysical property library coolprop. Ind Eng Chem Res 2014;53:2498–508.
[27] Declaye S. Improving the performance of micro-orc systems [Ph.D. thesis]. Liege, Belgium: University of Liege; 2015.

Please cite this article in press as: Guillaume L et al. Performance of a radial-inflow turbine integrated in an ORC system and designed for a WHR on truck application: An experimental comparison between R245fa and R1233zd. Appl Energy (2016), http://dx.doi.org/10.1016/j.apenergy.2016.03.012